Slovak Geol. Mag., 9,1 (2003), 65 – 75

Tourmaline-enriched horizons in the Lower Triassic quartzose sediments from the Tribeč Mts., Tatric Unit, Western Carpathians (Slovakia)

ANNA VOZÁROVÁ[1], JÁN JANOŠOV[1] and KATARÍNA ŠARINOVÁ[1]

[1]Departm. of Mineral. and Petrol., Faculty of Natural Science, Comenius University Bratislava, Mlynská dolina, pav. G, 842 15 Bratislava, Slovak Republic. Corresponding author: e-mail: vozarova@nic.fns.uniba.sk

Abstract. The tourmaline-rich laminae were found in the Lower Triassic Lúžna Fm. sediments of the Tatric Unit in the Tribeč Mts. Sedimentary features of the Lower Triassic sediments of the Tribeč Mts. Lúžná Fm. indicate the braided stream sedimentary model in semi-arid climatic conditions.

There were distinguished three varieties of tourmaline, two varieties of neomorphic tourmalines associated with clayey laminae, as well as clastic grains: 1. green/brown-green tourmaline with high degree of zonality, non-deformed by post-sedimentary tectonic deformation; 2. highly preferred aggregates of nearly unzonal green/green-bluish dravite-magnesiofoitite crystals, deformed by post-sedimentary foliation cleavage, together with primary clayey laminae; 3. well-rounded azonal clastic grains.

Chemical composition of the variety 1 tourmaline corresponds to alkali group with dravite-schorl-(foitite) end-member species. Generally, from the core toward to the rim is compositional zoning where Fe, Na, and Ti increase and Mg, Al decrease. Chemical composition of the variety 2 tourmaline corresponds generally to dravite species, rarely to magnesiofoitite. Mg^{2+} plays a dominant role at the Y-site occupancies in all the crystals. Slightly increasing of Mg/Fe ratio was found out within the scarce zonal tourmaline crystals of variety 2. Na is the dominant cation in the X-site on the both types of crystals and Ca, K concentration as well as Cr, Mn is very low or not detectable. Variety 3 tourmaline is compositionally monotonnous, corresponding to dravite species.

The following genesis for both neomorphic tourmaline varieties is supposed: A. variety 1: – fine-grained tourmaline detritus probably of several sources in the cores; – redistribution of boron as a result of post-depositional movement of boron-rich fluids in the rims; B. variety 2: – boron primarily attached to clay minerals and liberated during following process of diagenetic and low-grade metamorphic process. It is not excluded, that the primary clay laminae had been associated with presence of borates, genetically associated with small arid endorheic water reservoirs. C. variety 3: well-rounded clastic grains were derived from crystalline rocks complexes, mostly from mica schists and paragneisses coexisting with Al-saturating phase.

Key words: dravite, schorl, magnesiofoitite, Lower Triassic, quartzose sediments, Western Carpathians, braided alluvia

Introduction

Cropping out from the Tertiary sediments of the Danube Basin, the Tribeč Mts. represent the westernmost salient of the inner belt of the Western Carpathians Tatric Unit rock complexes. Generally, they consist of a crystalline core and their indigenous Late Paleozoic (mostly Permian) and Mesozoic envelope. The pre-Tertiary rock complexes of the Tribeč Mts. form a NE–SW striking horst divided by the Skýcov fault system into a northern Rázdiel part and a southern Zobor part (Fig. 1). Geological structure of the Tribeč Mts. comprises the crystalline basement of the Tatric and Veporic Unit and their Late Paleozoic-Mesozoic envelope sequences, the Late Paleozoic-Triassic assemblage of the Hronic Unit, as well as Tertiary and Quarternary sedimentary cover (Ivanička et al., 1998). The Tatricum crystalline rocks of the Zobor part are represented mainly by the granitoids of several petrographic types that make up a large, zonally structured Zobor pluton. The crystalline rocks of the Zobor part are direct unconformable overlapped by the Lower Triassic siliciclastic sequence. Generally, the Lower Triassic siliciclastic sequences were lithostratigraphically defined as the Lúžna Formation by Fejdiová (1980), formerly for the Tatric Unit, later also for the Fatric-Northern Veporic realm (Fejdiová, 1985; Vozárová and Fejdiová, 1996).

Lithological and depositional characteristics

The Lower Triassic of the Tribeč Mts. consists of sandstones (mainly coarse- to medium-grained) with intercalations of fine-grained conglomerates and inferior thin layers of silty/sandy shales. Generally, these sediments manifested their relatively high grade of structural and mineralogical maturity. In the Zobor part of the Tribeč Mts., as in prevalent part of the Tatric Unit, they occur in a new sedimentary cycle without direct connection to more polymictic (especially rich in feldspars) Permian deposits with synchronous acid volcanism. According to previous interpretation of Fejdiová (1980; 1985) sediments of the Lúžna Fm. correspond to marine litoral resp. barrier islands, deltas and shallow shelf depositional environment. Mišík & Jablonský (1978, 2000)

Slovak Geol. Mag., 9,1 (2003), 65 – 75

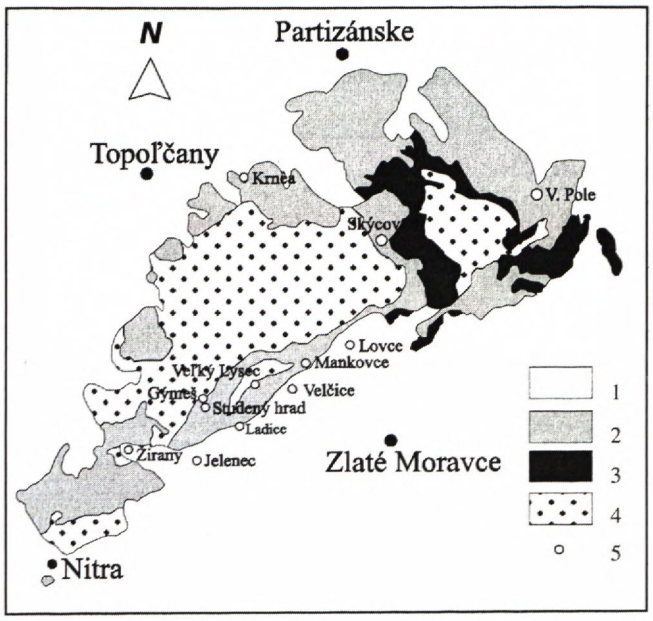

Fig. 1. Locations of investigated outcrops in the Tribeč Mts. Schematic geological map based on Ivanička et al (1998). Legend: 1 – Tertiary and Quarternary sediments; 2 – Mesozoic sedimentary rock complexes; 3 – Late Paleozoic sedimentary and volcanic rock complexes; 4 – Pre-Mesozoic crystalline rock complexes and magmatites; 5 – locations of investigated profiles of the Lower Triassic quartzose sediments.

interpreted the Lower Triassic of the Tatric Unit as continental sediments of ephemeral braided streams an a piedmont plain. Later, for the Lúžna Fm. sediments Fejdiová (in Ivanička et al., 1998) assumed a continental, fluvial sedimentary system. The eolian origin of the diagonal bedded sandstones from the Tribeč Mts. was postulated by Hók (1989). The braided stream depositional system is supposed for the Northern Veporic Lower Triassic sediments of the Čierťaž Mts. by Vozárová (2002).

The geometry of sedimentary bodies changes regionally and indicates the presence of laterally extensive drainage area. Single strata are very often lens- or wedge-shaped and tabular. The sedimentary complexes are represented predominantly by channel bars, consisting mostly of massive or horizontally bedded fine-grained conglomerates vertically replaced by coarse-grained sandstones with planar or trough cross-bedding (Fig. 2). In exposures sets of current bedding have apparent unimodal orientation (Pl. 1- Figs. 1, 2). Current planparallel horizontal lamination and cross-bedding is common in both type of these sediments. Contacts between individual bodies of channel bar sediments are often erosive, fringed with intraclasts of siltstones and claystones. The upper part of channel bars are represented by medium- to fine-grained sandstones, occasionally with ripple bedding (Pl.1- Fig. 3). The thickness of single channel sets is small, mostly not exceeding 2-2.5 m. These deposits correspond to migrating shallow channel bars in a river bed (longitudinal and transversal bars). Apart from these sediments, relics of channel fillings were identified. The filling consists of massive or horizontally bedded fine-grained conglomerates or coarse-grained sandstones with grain-supported structure. Transport directions derived from cross-bedding show a paleotransport from N. This data coincide well with those from the previous measurements of Hók (1989).

Sedimentary features of the Lower Triassic sediments of the Lúžná Fm. in the Tribeč Mts. indicate the braided stream sedimentary model in semi-arid climatic conditions. This sedimentary model is characterized by rivers with steep slope and relatively high speed of stream flow, that within a riverbed are split up into of shallow and broad channels, mutually divided by sandy or conglomerate accumulations and big floor dunes. The fluvial braidplain of ephemeral sandy-pebble streams was associated with intervals of strong aeolian activity. It was documented by occurrences of ventifacts (Pl. 1- Fig. 4) and layers of diagonally cross-bedded and structurally mature sandstones, with very good rounded grains.

Petrological characteristics

Conglomerates belong to oligomictic type, with absolute prevalence of quartz pebbles. Part of them have faceted clast shape (ventifact), attesting aeolian activity during the pauses of the stream transport (Mankovce; Pl. 1- Fig. 4). Quartz is dominant component among clasts: milky and pink varieties along with dark-pink, grey to black. It forms more than 90% of clasts, even in basal parts, while its concentration increases vertically and reaches more than 95% or up to 100% of all clasts. A substantial part of quartz pebbles is well roundned, suggesting mainly cyclic redeposition. However, entirely angular clasts of quartz occur too. Scarcely were identified pebbles of black tourmalinites and blastofelsitic acid volcanics. Besides them also clasts of graphitic metaquarzites were described by Mišík and Jablonský (2000) from Gýmeš.

Angular grains (4-5 mm in size) of pale-grey and beige K-feldspars represent a special detritic component in the basal conglomeratic layers of the Lower Triassic sequence. Intraclasts of violet, beige-red as well as green shales form a part of detritus, indicating processes of syndepositional erosion.

Sandstones predominantly belong to the group of quartzose arenites and subarcoses, with a high content of quartz grains (85–95 %), less K-feldspars (5–10%) and fragments of acid volcanites, clastic micas (muscovite and rarely secondary altered biotite) and heavy minerals. Small part of sandstones are compositionally with the affinity to sublitarenites, along with a relative higher felspars/acid volcanites ratio. Among heavy minerals were identified: zircon (2–30%), garnet (20–60%), ilmenite (7–18%), titanite (0–6%), rutile (1–5%), tourmaline (2–7%), magnetite (2–3), monazite-(Ce) (0.5–2.5%), rare epidote, goethite, anatase, allanite-(Ce) and gold (average of 3 analysis; bulk sample=15-20 kg).

Nearly all genetic types of quartz have been identified. Dominant are coarse-grained polycrystalline and monocrystalline as well as volcanogenic varieties, less occur fine-grained polycrystalline with preferred orientation and pressure-deformed cataclastic quartz grains. Occasionally, inclusions of muscovite, rarely rutile and

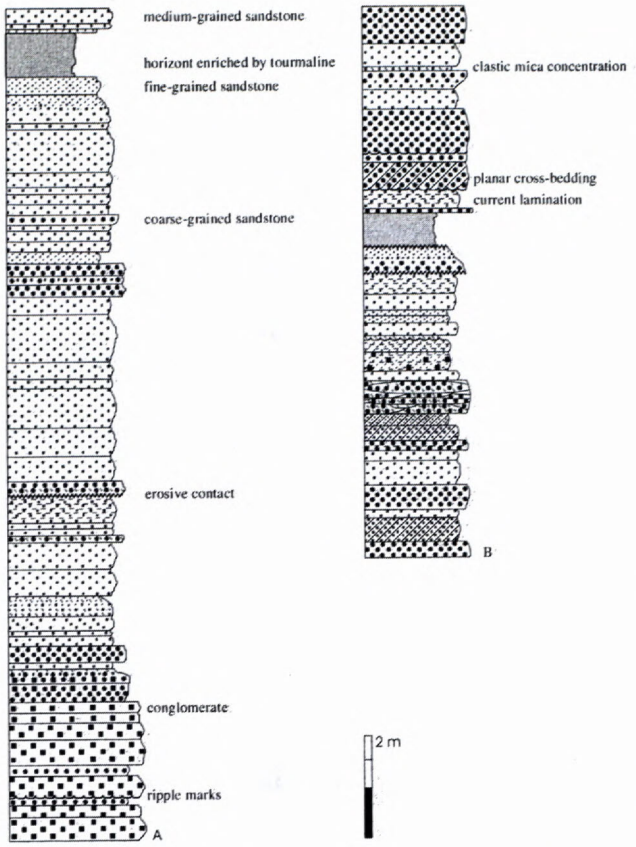

Fig. 2. Lithological log of Ladice (A) and Mankovce localities (B). Legend: 1 – conglomerate; 2 – coarse-grained sandstone; 3 – medium-grained sandstone; 4 – fine-grained sandstone; 5 – ripple marks; 6 – erosive contact; 7 – current lamination; 8 – planar cross-bedding; 9 – clastic mica concentration; 10 – horizons enriched by tourmaline.

zircon were detected in quartz grains. The surface of quartz grains is very often coated by Fe-oxides or very thin illite rim. Well roundned grains posses syntaxial quartz overgrowths (Pl. 1- Fig. 6).

Feldspars are almost exclusively orthoclase and more rarely microcline; perthite and plagioclase are very rare. K-feldspars are obviously clear, less of them cloudy due to different degree of kaolinization. They frequently preserved their tabular habitus as well as diagenetic syntaxial microcline overgrowths on older K-feldspars indented in quartz.

Besides of volcanic rocks small acid felsitic fragments with relics of spherulitic texture are common. They contain relics of beta-quartz type phenocrysts with magmatic corrosion.

The high grade of structural maturity is documented by a relatively low values of sorting, corresponding from well to moderate sorted sandstones (in the range of 0.35–0.7 *fi*, according to visual scale of Compton, 1962). The roudness of sandy grains reaches from 2.5 to 3.5 values, estimating subangular/subrounded and rounded grain shape (according to visual scale of Powers, 1953; Pl. 1- Fig. 6). Dominant are grains with spherical, subprismoidal and subdiscoidal shapes.

Primary clayey matrix is rare, only preserved as a recrystallized (quartzy-micaceous) partial filling of single pores. Very often are diagenetic coatings of micaceous or Fe-hydroxides minerals on the grain surfaces. Initially, clayey rim around quartz grains originated in the beginning of the early stage of diagenesis and it is older than the quartz cement that fills rest of pores between grains. The quartz cement occur in the forms of syntaxial cement or as a microcrystalline aggregate. Barite is very common among authigenic minerals in some localities.

The exceptionally phenomenon of the Lower Triassic sequence in the Tribeč Mts. are the tourmaline-bearing laminae. Besides of clastic tourmaline grains and tourmalinites clasts they were distinguished two type of neomorphic tourmalines: 1. green/brown-green tourmaline with high degree of zonality; single crystals have not been preferred oriented, but situated inside of primary clayey laminae; the individual crystals of tourmaline are not destructed by post-sedimentary tectonic deformation; 2. green/green-bluish tourmaline non-zonal, which forms high preferred aggregates of thin columnar crystals, parallel to sedimentary lamination; it is associated also with clayey laminae, but single crystals are deformed by post-sedimentary foliation cleavage together with primary clayey laminae (Pl. 1- Fig. 5). These two genetically different type of neomorphic tourmalines have also different chemical composition.

Chemical composition of tourmaline clasts as well as tourmaline crystals from clasts of tourmaline-rich rocks derived from the Lower Triassic sediments of the Tatric Unit was described by Uher (1999).

Analytical techniques

Electron microprobe analysis of tourmaline were performed on Cameca-SX 100 electron microprobe (operated with a beam current of 15 kV at 20 nA) at Slovak Geological Survey of Bratislava. The beam diameter is a 1-3 μm. The analytical data were reduced and corrected using the ZAF method. Anhydrous oxide and natural minerals were used as probe standards: wollastonite for Si Kα and Ca Kα , TiO_2 for Ti Kα, Al_2O_3 for Al Kα, hematite for Fe Kα, rhodonite for Mn Kα, MgO for Mg Kα, albite for Na Kα, orthoclase for K Kα, chromite for Cr Kα, BaF_2 for F Kα and NaCl for Cl Kα.

Characteristics of tourmaline

Based on available literature data (Henry and Guidotti, 1985; Hawthorne and Henry, 1999 and many others) tourmaline is shown to be a usefull petrogenetic indicator. Distinct composition field were defined within Al-Fe(tot)-Mg and Ca-Fe(tot)-Mg diagrams for tourmaline from three definied varieties. These tourmaline grains display three general styles of chemical zoning: 1. nearly/or lack of zoning; 2. core-to-rim zonation attributed to growth during progressive diagenesis and low-grade metamorphism; 3. detrital tourmaline grains non-zonal or sorrounded by a very thin metamorphic overgrowth.

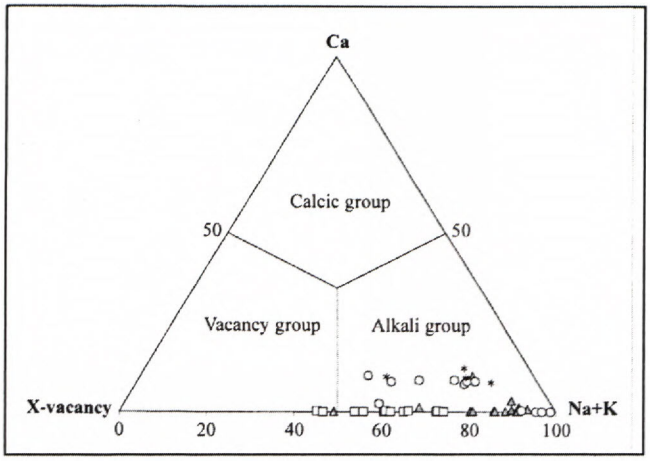

Fig. 3. Compositional diagram of tourmalines (after Hawthorne and Henry, 1999).
Legend: variety 1, subvariety a – circle; variety 1, subvariety b – triangle; variety 2 – square; variety 3 – asterisk.

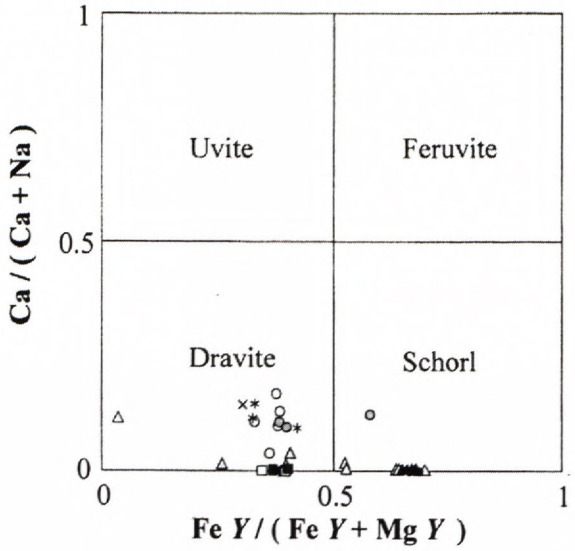

Fig. 4. Ca/(Ca+Na) vs. Fe/(Fe+Mg) diagram (atomic proportions) of varieties 1, 2 and 3 tourmalines.
Legend: variety 1, subvariety a – circle; variety 1, subvariety b – triangle; variety 2 – square; variety 3 – asterisk; core – rim = white - black.

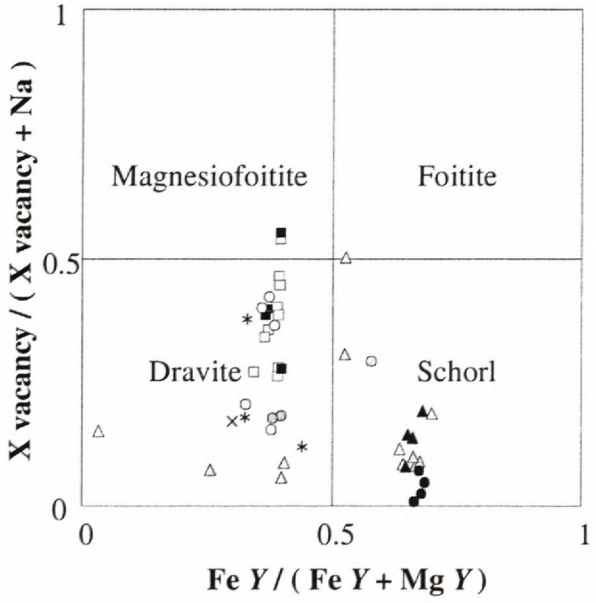

Fig. 5. X vacancy/(X vacancy+Na) vs. Fe/(Fe+Mg) diagram (atomic proportions) of varieties 1, 2 and 3 tourmalines. Legend: variety 1, subvariety a – circle; variety 1, subvariety b – triangle; variety 2 – square; variety 3 – asterisk; core – rim = white - black.

All of the studied samples contain Si-, Al and Ti-saturating phases (quartz and muscovite, new-formed rutile respectively).

Variety 1: Tourmaline crystals have a distinct chemical and optical zonation. They are concentrate within white mica-rich laminae, but crystals have not preferential orientation and they are irregularly disseminated within the individual laminae. Optically strongly zoned tourmaline crystals coexist with less amount of optically unzoned tourmaline crystals. The colour change may be gradational or involve sharp optical discontinuities. Some tourmaline grains showing these optical discontinuities have irregular cores overgrown by euhedral rims, whereas others have both euhedral cores and rims. Well rounded detritic cores are very scarce.

Chemical composition of the variety 1 tourmaline grains corresponds to alkali group with dravite-schorl end-member species (Tab. 1, Fig. 3). Generally, from the core toward to the rim is compositional zoning such that Fe, Na, and Ti increase as Mg and slightly also Al decrease. Variation in tourmaline 1 rim and core composition is more evident in changes of Fe/(Fe+Mg) ratios, ranging from 0.12 to 0.74. Among the tourmaline 1 crystals were observed slight compositional differences.The main differences are in X-site vacancies. Within the 1a subvariety Na is the dominant cation in the X-site (0.51-0.77 apfu for core, 0.90-0.96 apfu for rim) and Ca concentrations are generally low-lying (up to 0.10 apfu), but with decreasing trend at the X-site to the rim (Fig. 4). K is near detection limit of microprobe. Mn, Cr are also present in limited quantities. The W-site is occupied by mainly OH^{1-}, in small quantities substituted by F^{1-}. This tourmaline subvariety shows a relative strong decreasing in Al and Mg towards the rim (core: Fe/(Fe+Mg)=0.32-0.42, Al=5.80-6.00; rim: Fe/(Fe+Mg) =0.74-0.79, Al= 5.22-5.31). This trend is confirmed by the strong decreasing of alkali-defect substitution to the rim (Fig. 5). Generally, the 1b subvariety tourmalines show core-rim variability only in Fe-Mg compositionally zoning with distinct Mg decreasing to the rim (core to rim: Fe/ (Fe+Mg)=0.12 to 0.70, sample t1, Fig. 4, 5, 6, 7). Substitution in 1b tourmaline can take place as homovalent cation exchanges on the Y-site (Fe^{2+} for Mg^{2+}).

Variety 2: Tourmaline is found as an euhedral, thin-columnar crystals, that are disseminated in a white mica-rich thin layers. Tourmaline crystals are distinct preferential oriented, parallel to crystallization schistosity and deformed by crenulation cleavage (Pl. 1- Fig. 5). They form laminae up to 5 mm thick. These textural relations suggest that there have been some overgrowths on pre-existing boron-rich sedimentary laminae as well as nucleation

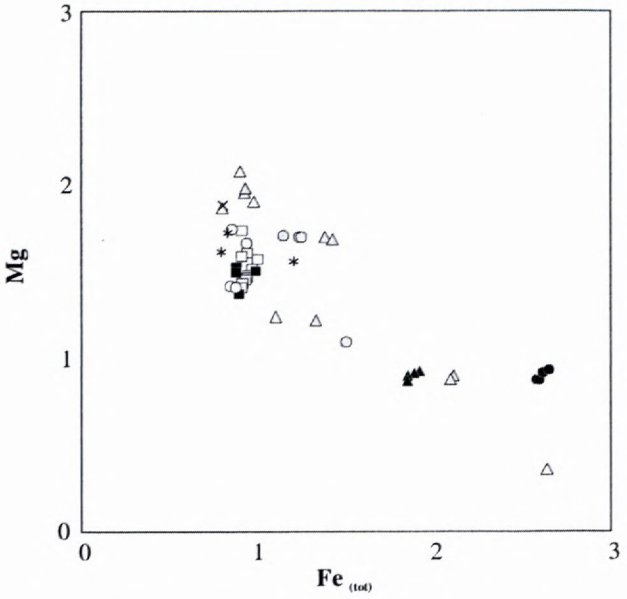

Fig. 6. Mg vs. Fe diagram (atomic proportions) of varieties 1, 2 and 3 tourmalines. Legend: variety 1, subvariety a – circle; variety 1, subvariety b – triangle; variety 2 – square; variety 3 – asterisk; core – rim = white - black.

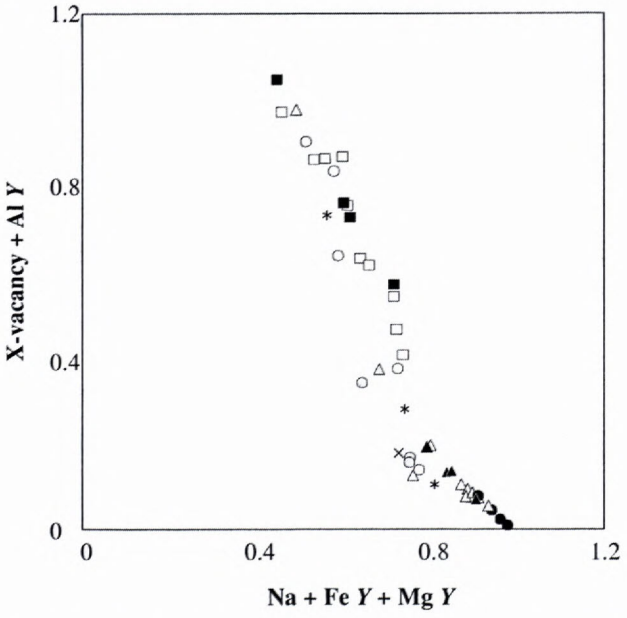

Fig. 7. X vacancy+^{Y}Al vs. ^{X}Na+^{Y}(Fe +Mg) diagram (atomic proportion) of varieties 1, 2 and 3 tourmalines. Legend: variety 1, subvariety b – triangle, variety 2 – square, variety 3 – asterisk, core – rim = white - black..

and growth of new tourmaline during process of authigenesis and following metamorphism.

Chemical composition of the variety 2 tourmaline corresponds generally to dravite (Figs. 3). Looking at the occupancies of Y-site, Mg^{2+} plays a dominant role in all the samples (Mg=1.37-1.73 apfu.). Mg/Fe ratio varies in of 1.55-1.90 (mean 1.67; n=6) in the unzonal tourmaline crystals. Representative microprobe analyses of the variety 2 are presented in Table 2.

Slightly increasing of Mg/Fe ratio was found out within the scarce zonal tourmaline crystals: ***core*** (range 1.53-1.56; mean 1.55; n=4), ***rim*** (range 1.52-1.72; mean 1.62; n=4). Na is the dominant cation in the X-site on the variety 2 tourmalines and Ca concentration is very low or not detectable (Fig. 4). Substitution in variety 2 tourmaline is heterovalent, coupled substitutions Mg-Fe in Y-site and alkali-defect substitution in X-site (Fig. 5, 6, 7). Some variety 2 tourmaline crystals have the end-member composition of magnesiofoitite. The end-member composition of magnesiofoitite was given with a variable cation occupancy at Y-site: Y-site is occupied by [Mg_2Al] (MacDonald et al. 1993; Hawthorne and Henry, 1999).

Variety 3: It is represented by clastic tourmaline grains within heavy mineral fraction. They are very good rounded, optical unzoned and/or with very thin metamorphic overgrowths on their surface. Compositionally are monotonnous, corresponding to dravite species with Fe/(Fe+Mg) in the range of 0.33-0.44, Al=5.91-6.00 and dominant Na on Y-site, with minor or not detectable amount of Ca and K (Tab. 2).

Discussion

Looking on the discrimination diagrams Al-Fe(tot)-Mg and Ca-Fe(tot)-Mg (Figs. 8, 9, 10, 11) of Henry and Guidotti (1985) two distinct core-rim trends can be recognized within the tourmaline of variety 1 (Figs. 8, 9). These zoned tourmalines have a complex history. They are differences in core and in rim compositions between subvarieties 1a and 1b. Samples nt 2 and nt 5 show distinct core-rim decreasing trend of Mg and Al, which indicates substitutions Mg-Fe in Y-site (Fig. 6, 10) and Na for vacancy in X-site (Fig. 5). The data of sample t1, within 1b tourmaline (Fig. 9) cluster along a line of nearly constant Al content and slightly Fe^{3+}- rich correlating with field (6). On the other hand, sample nt 2, nt 3 cores signalize increasing alkali-defect substitution, corresponding to the coexistence with Al-saturating phase (Fig. 8). As evidenced by the large variability of composition, both type of cores show considerably more compositional variation than corresponding rim composition. Instead of this, the tourmaline rims from both samples are compositionally equal. They are in chemical equilibrium with the matrix phases, which correspond to P-T condition of metamorphism. According to Henry and Guidotti (1985) discrimination diagrams (Fig. 10, 11) the core-rim compositions correspond from coexisting and/or not-coexisting Al-saturating phase to tourmaline from Li-poor granitoids and their associated pegmatites and aplites. A slight variability of core-Ca content between subvariety 1a and 1b can be caused by differences in primary matrix material (alternating of Ca enriched and Ca poor laminae of pelite). Different core-rim composition in variety 1 tourmalines is most probably effect of different source of boron: 1. fine-grained tourmaline detritus probably of several sources in the cores; 2. redistribution of boron as a result of post-sedimentary and pos-deformational movement of boron-rich fluids in the rims.

Tab.1. Representative microprobe analyses of variety 1a, b tourmalines from the Lower Triassic quartzites of Tribeč Mts.
** - B_2O_3 and H_2O contents of the minerals calculated by ideal stoichiometry (3 boron cations and OH+F+Cl = 4 anions). n.d. - non-detectable.*

	variety 1a						variety 1b					
sample	nt1a	nt1b	nt1c	nt5a	nt5b	nt5c	t1a	t1b	t1c	t1d	t1e	t1f
position	core	zone 1	rim	core	zone 1	rim	core	zone 1	zone 2	zone 3	zone 4	rim
SiO_2	36.83	36.47	35.32	37.96	36.59	35.39	38.29	36.71	37.11	36.64	35.99	36.35
TiO_2	1.19	1.24	1.18	0.06	0.50	1.39	0.90	0.68	0.36	0.06	1.13	1.20
Al_2O_3	29.98	29.72	25.77	32.98	30.73	25.92	30.49	29.37	29.56	29.12	28.64	29.19
B_2O_3 *	10.58	10.49	9.99	10.81	10.53	10.03	10.90	10.48	10.51	10.38	10.24	10.32
Cr_2O_3	0.01	0.02	0.02	0.00	0.04	0.01	0.00	0.02	0.03	0.05	0.01	0.01
MgO	6.92	6.84	3.51	6.89	6.90	3.38	11.05	6.83	7.99	6.74	3.44	3.61
FeO	8.98	8.96	17.93	6.95	8.45	17.74	2.75	9.93	7.69	10.20	14.65	13.34
CaO	0.49	0.48	0.02	0.13	0.45	0.00	0.57	0.05	0.06	0.17	0.00	0.01
MnO	0.03	0.00	0.00	0.00	0.00	0.05	0.00	0.01	0.01	0.00	0.03	0.03
Na_2O	2.42	2.34	2.68	1.88	2.34	2.86	2.55	2.89	2.83	2.73	2.72	2.76
K_2O	0.01	0.01	0.07	0.00	0.00	0.04	0.01	0.01	0.02	0.01	0.07	0.06
H_2O *	3.57	3.56	3.43	3.73	3.59	3.40	3.76	2.80	2.93	2.70	2.35	2.46
F	0.17	0.11	0.04	0.00	0.09	0.13	n.d.	n.d.	n.d.	n.d.	n.d.	n.d.
CL	0.00	0.01	0.01	0.00	0.00	0.00	0.00	0.00	0.01	0.00	0.00	0.00
O=F	-0.07	-0.05	-0.02	0.00	-0.04	-0.06	n.d.	n.d.	n.d.	n.d.	n.d.	n.d.
O=Cl	0.00	0.00	0.00	0.00	0.00	0.00	0.00	0.00	0.00	0.00	0.00	0.00
TOTAL	101.10	100.20	99.95	101.38	100.17	100.29	101.27	99.98	99.11	99.88	99.27	99.34
Formulae based on the 31 anions												
Si	6.048	6.044	6.142	6.104	6.041	6.131	6.107	6.087	6.134	6.103	6.106	6.125
Al T	0.000	0.000	0.000	0.000	0.000	0.000	0.000	0.000	0.000	0.000	0.000	0.000
Total T	6.048	6.044	6.142	6.104	6.041	6.131	6.107	6.087	6.134	6.103	6.106	6.125
B	3.000	3.000	3.000	3.000	3.000	3.000	3.000	3.000	3.000	3.000	3.000	3.000
Al Z	5.803	5.804	5.282	6.000	5.979	5.292	5.731	5.740	5.759	5.716	5.726	5.797
Fe Z	0.197	0.196	0.718	0.000	0.021	0.708	0.269	0.260	0.241	0.284	0.274	0.203
Total Z	6.000	6.000	6.000	6.000	6.000	6.000	6.000	6.000	6.000	6.000	6.000	6.000
Ti Y	0.147	0.155	0.154	0.007	0.062	0.181	0.108	0.085	0.044	0.071	0.144	0.152
Al Y	0.000	0.000	0.000	0.254	0.000	0.000	0.000	0.000	0.000	0.000	0.000	0.000
Cr	0.001	0.002	0.002	0.000	0.005	0.002	0.000	0.003	0.004	0.007	0.002	0.001
Fe Y	1.036	1.046	1.890	0.935	1.146	1.862	0.097	1.117	0.822	1.137	1.804	1.677
Mn	0.004	0.000	0.000	0.000	0.000	0.007	0.000	0.002	0.001	0.000	0.004	0.004
Mg	1.694	1.690	0.911	1.652	1.697	0.872	2.627	1.689	1.969	1.675	0.870	0.908
Total Y	2.882	2.893	2.957	2.848	2.910	2.924	2.832	2.896	2.840	2.890	2.824	2.742
Ca	0.086	0.085	0.004	0.023	0.079	0.000	0.097	0.008	0.010	0.031	0.000	0.002
Na	0.772	0.751	0.903	0.585	0.750	0.961	0.760	0.930	0.907	0.881	0.896	0.900
K	0.001	0.002	0.016	0.000	0.001	0.009	0.003	0.003	0.005	0.002	0.015	0.014
Total X	0.859	0.838	0.923	0.608	0.830	0.970	0.860	0.941	0.922	0.914	0.911	0.916
X - vacancy	0.141	0.162	0.077	0.392	0.170	0.030	0.140	0.059	0.078	0.086	0.089	0.084
OH	3.913	3.944	3.979	4.000	3.952	3.928	4.000	3.999	3.997	4.000	4.000	4.000
F	0.087	0.059	0.023	0.000	0.048	0.073	n.d.	n.d.	n.d.	n.d.	n.d.	n.d.
Cl	0.000	0.003	0.002	0.000	0.000	0.001	0.000	0.001	0.003	0.000	0.000	0.000
Total V+W	4.000	4.000	4.000	4.000	4.000	4.000	4.000	4.000	4.000	4.000	4.000	4.000
Fe/Fe+Mg	0.421	0.424	0.741	0.361	0.407	0.747	0.122	0.449	0.351	0.459	0.705	0.674

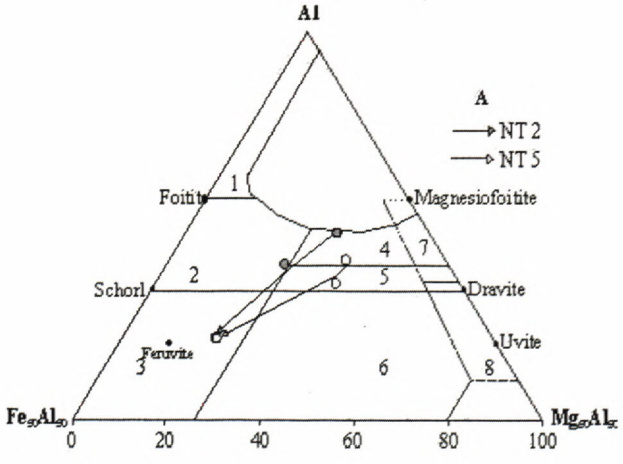

Fig. 8.Trend of zoning in the tourmaline of subvariety 1a. Arrows show changes from core to rim. Fields after Henry and Guidotti (1985): 1. Li-rich granitoid pegmatites and aplites; 2. Li-poor granitoids and their associated pegmatites and aplites; 3. Fe^{3+}-rich quartz-tourmaline rocks (hydrotermally altered granites); 4. Metapelites and metapsamites coexisting with an Al-saturating phase; 5. Metapelites and metapsamites not coexisting with Al-saturating phase; 6. Fe^{3+}-rich quartz-tourmaline rocks, calc-silicate rocks and metapelites; 7. Low-Ca metaultramafics and Cr, V-rich metasediments; 8. meta-carbonates and meta-pyroxenites. Legend: variety 1, subvariety a – circle; variety 1, subvariety b – triangle; variety 2 – square; variety 3 – asterisk.

*Tab. 2. Representative microprobe analyses of variety 2 and 3 tourmalines from the Lower Triassic quartzites of Tribeč Mts. * - B_2O_3 and H_2O contents of the minerals calculated by ideal stoichiometry (3 boron cations and OH+F+Cl = 4 anions).*

	variety 2				variety 3	
sample	JS1a	JS1b	JS3a	JS3b	tk3a	tk3b
position	core	rim	core	rim	core	rim
SiO_2	37.49	37.64	37.54	37.67	36.88	37.37
TiO_2	0.16	0.17	0.34	0.44	0.73	0.77
Al_2O_3	33.43	34.02	32.83	33.54	30.41	31.62
B_2O_3 *	10.64	10.72	10.72	10.77	10.52	10.74
Cr_2O_3	0.00	0.00	0.02	0.00	0.06	0.04
MgO	5.75	5.66	6.23	6.21	6.28	7.74
FeO	6.70	6.63	7.12	6.49	8.73	5.97
CaO	0.00	0.01	0.00	0.01	0.46	0.70
MnO	0.00	0.00	0.00	0.00	0.04	0.00
Na_2O	1.45	1.42	2.27	1.92	2.52	2.31
K_2O	0.03	0.04	0.06	0.05	0.02	0.03
H_2O *	3.63	3.61	3.56	3.66	2.90	3.26
F	0.08	0.19	0.28	0.13	n.d.	n.d.
CL	0.01	0.00	0.01	0.01	0.00	0.00
O=F	-0.03	-0.08	-0.12	-0.05	n.d.	n.d.
O=Cl	0.00	0.00	0.00	0.00	0.00	0.00
TOTAL	99.34	100.03	100.86	100.84	99.55	100.55
Formulae based on the 31 anions						
Si	6.126	6.104	6.086	6.076	6.092	6.048
Al T	0.000	0.000	0.000	0.000	0.000	0.000
Total T	6.126	6.104	6.086	6.076	6.092	6.048
B	3.000	3.000	3.000	3.000	3.000	3.000
Al Z	6.000	6.000	5.914	5.924	5.920	6.000
Fe Z	0.000	0.000	0.000	0.000	0.080	0.000
Total Z	6.000	6.000	6.000	6.000	6.000	6.000
Ti Y	0.020	0.021	0.041	0.053	0.090	0.094
Al Y	0.438	0.502	0.359	0.452	0.000	0.031
Cr	0.000	0.000	0.002	0.000	0.008	0.005
Fe Y	0.916	0.899	0.965	0.876	1.125	0.809
Mn	0.000	0.001	0.000	0.000	0.005	0.000
Mg	1.401	1.369	1.506	1.493	1.547	1.868
Total Y	2.775	2.792	2.873	2.874	2.775	2.807
Ca	0.000	0.002	0.001	0.002	0.082	0.121
Na	0.460	0.446	0.714	0.599	0.806	0.724
K	0.007	0.008	0.012	0.011	0.004	0.007
Total X	0.467	0.456	0.727	0.612	0.892	0.852
X - vacancy	0.533	0.544	0.273	0.388	0.108	0.148
OH	3.959	3.901	3.860	3.939	4.000	3.999
F	0.043	0.099	0.143	0.064	n.d.	n.d.
Cl	0.002	0.000	0.003	0.003	0.000	0.001
Total V+W	4.000	4.000	4.000	4.000	4.000	4.000
Fe/Fe+Mg	0.395	0.396	0.391	0.370	0.438	0.302

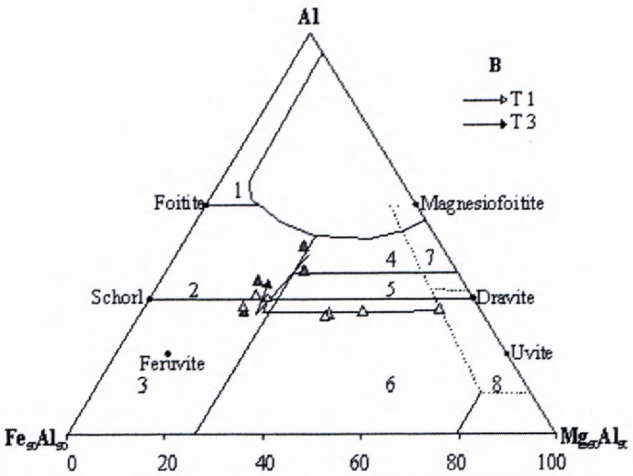

Fig. 9. Trend of zoning in the tourmaline of subvariety 1b. Arrows show changes from core to rim. Explanations as Fig. 8.

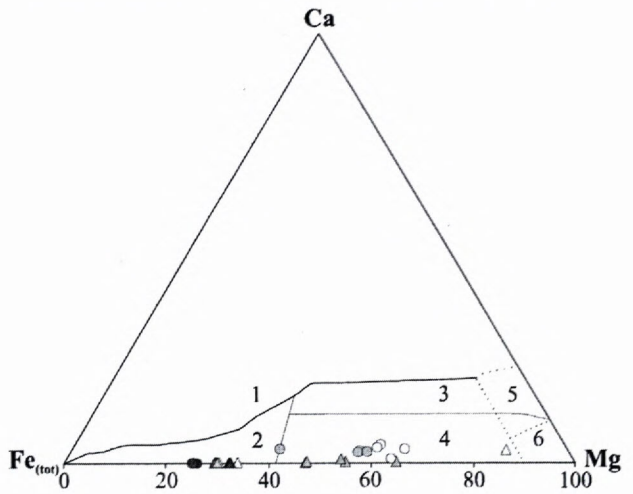

Fig. 10. Ca-Fe(tot)-Mg diagram (atomic proportions) tourmaline subvarieties 1a and 1b (core – rim = white – black). Fields after Henry and Guidotti (1985)): (1) Li-rich granitoid pegmatites and aplites; (2) Li-poor granitoids and associated pegmatites and aplites; (3) Ca-rich metapelites, metapsammites, and calc-silicate rocks; (4) Ca-poor metapelites, metapsammites, and quartz-tourmaline rocks; (5) Metacarbonates; (6) Metaultramafics. Legend: variety 1, subvariety a – circle; variety 1, subvariety b – triangle; variety 2 – square; variety 3 – asterisk; (+ - overgrowth on the clastic grain).

Comparing to the above mentioned, the tourmaline of variety 2 shows a relatively homogenous chemical composition (Figs. 4, 5, 12, 13), with high Mg/Fe ratios and negligible Ca content but relatively higher Al concentrations. This variety is corresponding to dravite species, rarely to magnesiofoitite. Dominant is alkali-vacant substitution in X-site (Fig. 5, 7). It corresponds to tourmaline associated with the compositional range of metapelites and metapsamites coexisting with an Al-saturating phase (Fig. 12, 13). The tourmaline-muscovite laminae indicates the primary clay-rich environment enriched in boron. The boron apparently was in solution within small areas of endorheic lake water in the semi-arid braided alluvial plain. It was held by adsorption onto the surface of clay minerals (substitution for silicon in the tetrahedral sites of the clay minerals). During prograding diagenetic process, the boron was released from the clays and made available to interstical fluids to react with the coexisting alumosilicate minerals in the sediments to form authigenic tourmaline. Further increase in temperature, causing boron releasing and forming of additional tourmaline zone on the preexisting core. The slight compositionally changes show minimal core-rim increasing in Al and Fe. Tourmaline of dravite composition, with most notable compositionally Fe-Al variations and less X-site vacancy was described from the cap rock of a salt dome (Gulf of Mexico) by Henry et al. (1999).

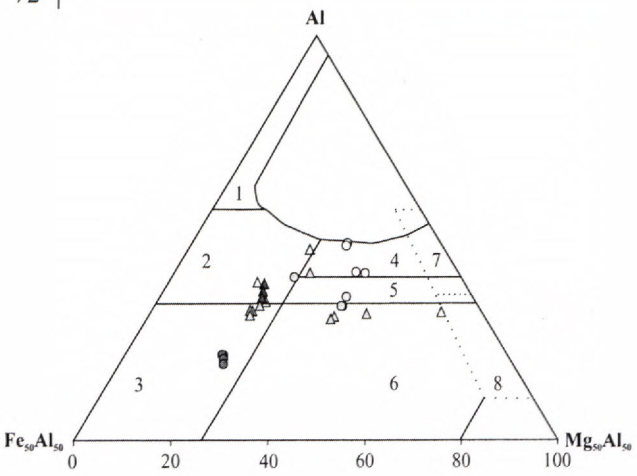

Fig. 11. Al-Fe(tot)-Mg diagram (atomic proportion) tourmaline subvarieties 1a and 1b (core–rim = white–black).
Explanations and symbols as Fig. 8 (× - overgrowth on the clastic grain).

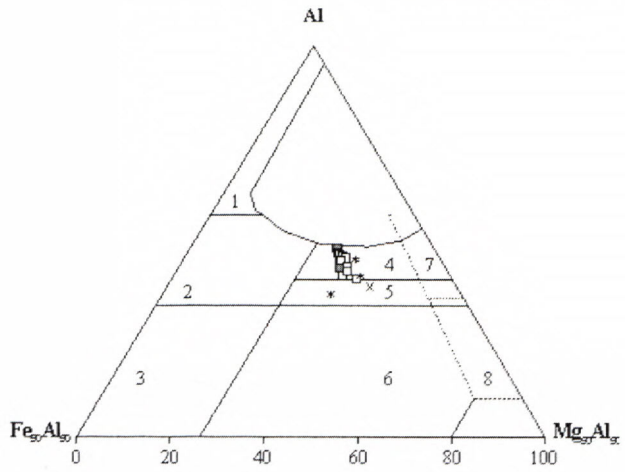

Fig. 13. Al-Fe(tot)-Mg diagram (atomic proportion) tourmaline varieties 2 and 3 (core–rim = white–black).
Explanations and symbols as Fig. 8 (× - overgrowth on the clastic grain).

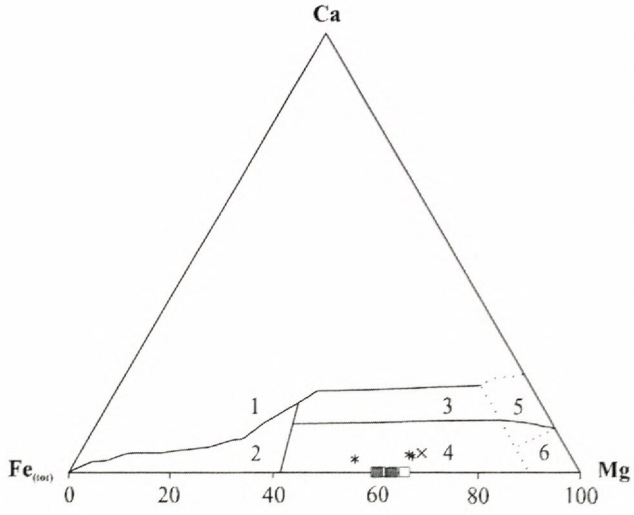

Fig. 12. Ca-Fe(tot)-Mg diagram (atomic proportions) tourmaline varieties 2 and 3 (core – rim = white – black).
Explanations and symbols as Fig. 10.

It could be also expected, that fluviatile concentration of water in separated small endorheic basins was associated with a strong evaporation during an arid climatic event. In this specific conditions the clays could have beeen altered in a concentrating brines. Boron was primarily attached to clay minerals and was liberated during following process of decomposition in concentrating brines. When the clays are altered in hypersaline bitterns to mixed-layer varieties rich in Mg, the original lattices are destroyed and boron is liberated (Sonnenfeld, 1984). The liberated boron could form also an independent laminae of primary borates associated with clay lamination. If this expectation is valid, then the genesis of the tourmaline laminae could be associated with primary borate-clay laminae.

Tourmaline of variety 3 is represented by very often clastic dravite grains. Compositionally has proximity to variety 2 but is more variably in Ca content. The variety 3 mainly correspond to tourmaline derived from metapelites and metapsamites with Al-saturating phase. Since the grains are non-zonal, the source area could be in crystalline rock complexes (mica schist/paragneisses terrane).

Conclusions

The tourmaline-rich laminae were found in the Lower Triassic Lúžna Fm. sediments of the Tatric Unit in the Tribeč Mts. Sedimentary features of the Lower Triassic sediments of the Lúžna Fm. in the Tribeč Mts. indicate the braided stream sedimentary model in semi-arid climatic conditions. The fluvial braidplain of ephemeral sandy-pebble streams was associated with intervals of aridity with a strong aeolian activity.

There were distinguished three type, from which two varieties belong to neomorphic tourmaline: *variety 1:* green/brown-green tourmaline with high degree of zonality, associated with primary clayey laminae and non-deformed by post-sedimentary tectonic deformation; *variety 2:* high preferred agregates of nearly non-zonal green/green-bluish tourmaline crystals, deformed by post-sedimentary foliation cleavage together with primary clayey laminae; *variety 3:* well-rounded clastic dravite grains. These two genetically different type of neomorphic tourmaline have also different chemical composition.

Chemical composition of the variety 1 tourmaline corresponds to alkali group with dravite-schorl-(foitite) end-member species. Generally, from the core toward to the rim is compositional zoning such that Fe, Na, and Ti increase as Mg and slightly also Al decrease. This is signalizing substitutions Mg-Fe in Y-site and Na in X-site vacancy. Chemical composition of the variety 2 tourmaline corresponds generally to dravite, rarely to magnesiofoitite. Mg^{2+} plays a dominant role at the Y-site occupancies in all the samples. Slightly increasing of Mg/Fe ratio was found out within the scarce zonal tourmaline crystals of variety 2. Dominant is alkali-vacant substitution in X-site.

Na is the dominant cation in the X-site on the both types and Ca, K concentration as well as Cr, Mn is very low or not detectable.

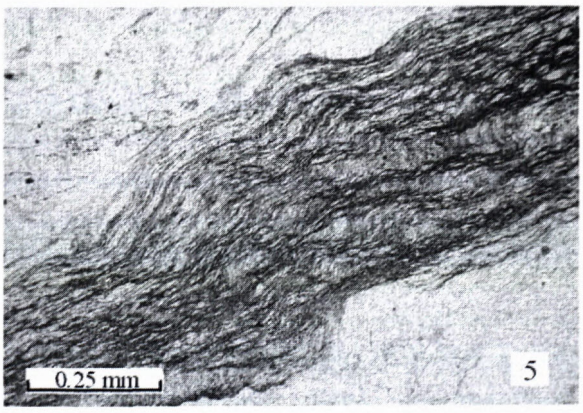

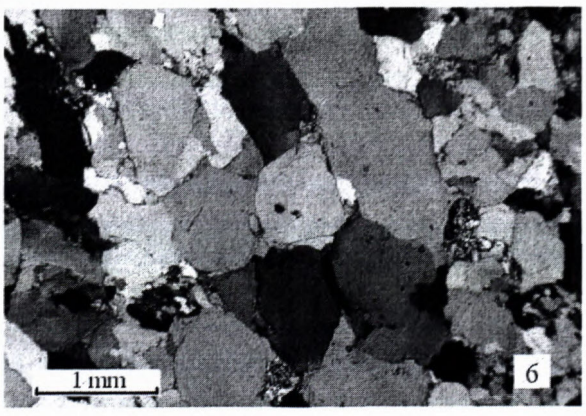

Plate 1.

Fig. 1. Planar angular cross-bedding (Studený vrch), Fig. 2. Planar tangential cross-bedding (Studený vrch), Fig. 3. Asymetric ripple marks on the bedding surface (Mankovce), Fig. 4. Faceted clast (venticlasts) indicates aeolian activity during the pauses of stream transport (Mankovce), Fig. 5. Laminae of tourmaline variety 2, Fig. 6. Well-rounded clastic quartz grains with syntaxial cement. X pollars

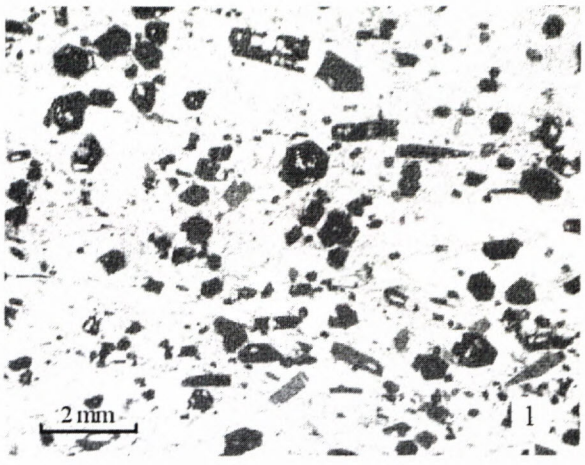

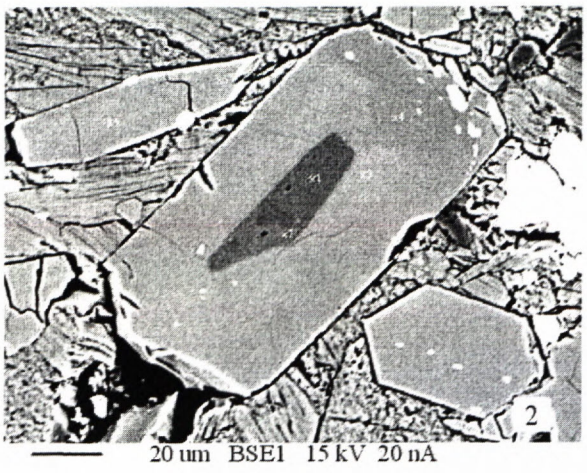

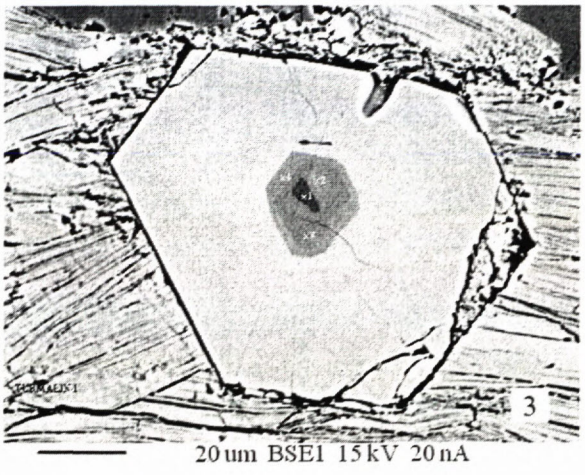

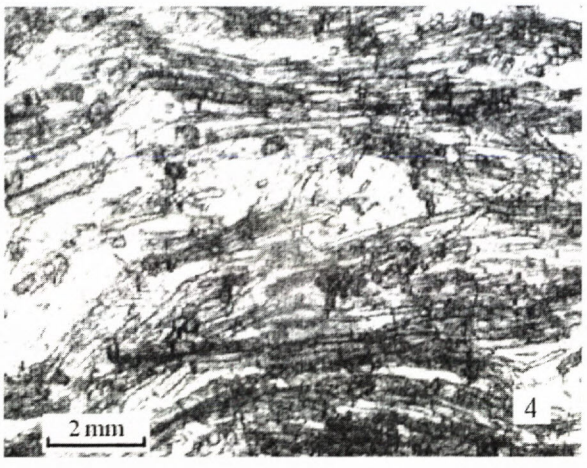

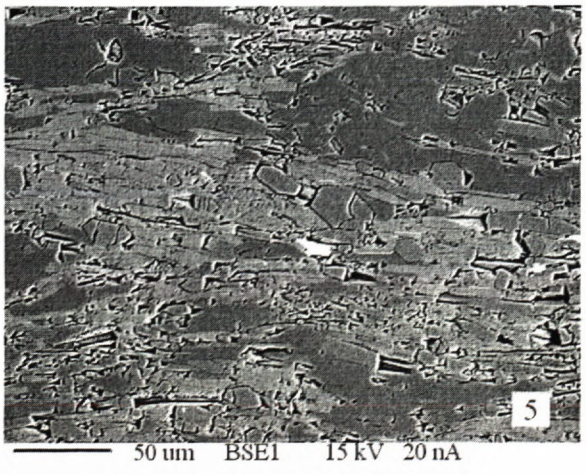

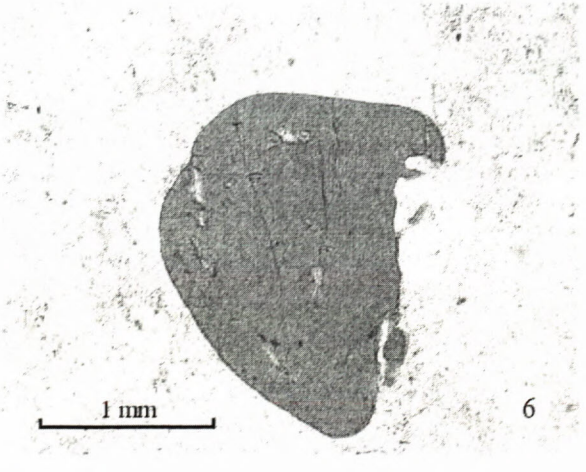

Plate 2.

Fig.1. Lamina with disordered variety 1 toumalines. Microphoto, || polars. Jelenec, Fig. 2. BSE image of variety 1 tourmaline (subvariety 1a) with rutile inclusions associated with matrix white mica (Žirany), Fig. 3. BSE image of variety 1 tourmaline (subsubvariety 1b) associated with white mica groundmass (Žirany), Fig. 4. Well preferred crystals of variety 2 tourmaline. || polars. Jelenec, Fig. 5. BSE image of variety 2 tourmaline crystals associated with white mica and quartz as a matrix minerals (Jelenec), Fig. 6. Optical microphoto showing well rounded clastic grain of variety 3 tourmaline. || polars. Mankovce.

The following genesis for the both neomorphic tourmaline varieties is supposed: A. variety 1: - fine-grained tourmaline detritus probably of several sources in the cores; - redistribution of boron as a result of post-depositional movement of boron-rich fluids in the rims; B. variety 2: - boron primarily attached to clay minerals and liberated during following process of diagenetic and low-grade metamorphic process. It is not excluded, that the primary clay laminae had been associated with presence of borates, genetically associated with small arid endorheic water reservoirs.

Clastic grains of the variety 3 tourmaline represent dravite, derived probably from crystalline rocks complexes, mostly from mica schists and paragneisses coexisting with Al-saturating phase.

Acknowledgements

The authors thanks to Dr. Pavel Uher for their comments and suggestions. This research was supported by Grant Project of No. 1/8205/01 of the Scientific Grant Agency of Ministry of Education of Slovak Republic and Slovak Academy of Sciences, Commission VEGA no. 3, on Science of Earth and Cosmos.

References

Compton, R. R., 1962: Manual of Field Geology. New York: Willey. 1-214.

Fejdiová, O., 1980: Liptovská Lúžna Sequence – formal Lower Triassic lithostratigraphic unit. Geol. Práce, Správy 74, 85-95 (in Slovak).

Fejdiová, O., 1985: New information on Lower Triassic Lúžna Clastic Formation in the Central Western Carpathians. Záp. Karpaty, Sér. Min., Petr., Geochem., Lož., 10, 111-160, (in Slovak, Engl. Res.).

Hawthorne, F. C. & Henry, D. J., 1999: Classification of the minerals of the tourmaline group. *Eur. J. Mineral.*, Vol. 11, 201-215.

Henry, D. J. & Guidotti, V. Ch., 1985: Tourmaline as a petrogenetic indicator mineral: an example from the staurolite-grade metapelites of NW Maine. Americ. Mineral., Vol. 70, 1-15.

Henry, D. J., Kirkland, B. I. & Kirkland, D. W., 1999: Sector-zoned tourmaline from the cap rock of salt dome. Eur. J. Mineral., 11, 263-280.

Hók, J., 1989: Paleocurrent analysis and genesis of Lúžna Beds in SE part of Tribeč Mts. Region. Geol. Záp. Karpát, 25, 137-141 (in Slovak, with Engl. Res.).

Ivanička, J. (Ed.), Hók, J., Polák, M., Határ, J., Vozár, J., Nagy, A., Fordinál, K., Pristaš, J., Konečný, V., Šimon, L., Kováčik, M., Vozárová, A., Fejdiová, O., Marcin, D., Liščák, P., Macko, A., Lanc, J., Šantavý, J. & Szalayová, V., 1998: Explanation to geological map of the Tribeč Mts., 1:50 000. Geol. Surv. Slovak Republic, D. Štúr Publ., Bratislava, 1-247 (in Slovak, Engl. Res.).

MacDonald, D. J., Hawthorne, F. C. & Grice, J. D., 1993: Foitite, $\square[Fe^{2+}(Al,Fe^{3+})]Al_6Si_6O_{18}(BO_3)_3(OH)_4$, a new alkali-deficient tourmaline: description and crystal structure. Am. Mineral., 78, 1299-1303.

Mišík, M. & Jablonský, J., 1978: Lower Triassic quartzites and conglomerates in Malé Karpaty Mts. (pebble analysis, transport direction, genesis). Acta Geol. Geogr. Univ. Comen., 33, 5-36 (in Slovak, Germ. Res.).

Mišík, M. & Jablonský, J., 2000: Lower Triassic quartzites of the Western Carpathians: transport directions, source of clastics. Geol. Carpath., 51, 251-264.

Powers, M. C., 1953: A new roudness scale for sedimentary particles. Journ. Sediment. Petrology, 23, 117-119.

Sonnenfeld, P., 1984: Brines and Evaporites. Acad. Press, Inc., Orlando, 1-613.

Uher, P., 1999: Clasts of tourmaline-rich rocks in Lower Triassic quartzites, the Tatric Unit, Central Western Carpathians: tourmaline composition and problem of source area. Geol. Carpath., Spec. Iss. 50, 140-141.

Vozárová, A., 2002: The braided stream depositional system in Lower Triassic of the Northern Veporicum (Western Carpathians, Slovakia). Geol. Carpath., Spec. Iss., 53, 52-54.

Vozárová, A. & Fejdiová, O., 1996: Beginning of Mesozoic sedimentary cycle. Geol. Práce, Spr., 101, 36-37.

Appendix

List of investigated localities:

Gýmeš – natural outcrop; fine-grained oligomictic conglomerates; tourmaline: variety 3;

Jelenec – abandoned quarry; cyclical quartzose sediments consist of coarse- to fine-grained sandstones, with less thin intercalations of fine-grained conglomerates in the basal part and siltstones and pelites in the upper part of the sequence; tourmaline: variety 1, 2 and 3;

Krnča – quarry; cyclical quartzose sediments consist of coarse- to fine-grained sandstones, with less thin intercalations of fine-grained conglomerates in the basal part and siltstones and pelites in the upper part of the sequence; tourmaline: variety 1 and 3;

Ladice – abandoned quarry; cyclical quartzose sediments consist of coarse- to fine-grained sandstones, with less thin intercalations of fine-grained conglomerates in the basal part and siltstones and pelites in the upper part of the sequence; tourmaline: variety 1 and 3;

Mankovce – abandoned quarry; cyclical quartzose sediments consist of coarse- to fine-grained sandstones, with less thin intercalations of fine-grained conglomerates in the basal part and siltstones and pelites in the upper part of the sequence; tourmaline: variety 1 and 3;

Skýcov – nature outcrop; cyclical alternation of fine-grained oligomictic conglomerates and coarse-grained quartzose sandstones; tourmaline: variety 3;

Studený hrad – natural outcrop; coarse-grained quartzose sandstones; tourmaline: variety 3;

Veľký Lysec – natural outcrop; coarse- to medium-grained quartzose sandstones; tourmaline: variety 3;

Velčice – small quarry; medium-grained quartzose sandstones; tourmaline: variety 3;

Velčice – large quarry; alternation medium- to fine grained quartzose sandstones; tourmaline: variety 1 and 3;

Žirany – abandoned quarry; cyclical quartzose sediments consist of coarse- to fine-grained sandstones, with less thin intercalations of fine-grained conglomerates in the basal part and siltstones and pelites in the upper part of the sequence; tourmaline: variety 1 and 3.